

# ASCA Observations of Two Ultra-Luminous Compact X-Ray Sources in the Edge-on Spiral Galaxy NGC 4565

Tsunefumi MIZUNO, Tomohisa OHNISHI, Aya KUBOTA, Kazuo MAKISHIMA,  
and Makoto TASHIRO

*Department of Physics, University of Tokyo, 7-3-1 Hongo, Bunkyo-ku, Tokyo 113-0033*

*E-mail(TM): mizuno@amalthea.phys.s.u-tokyo.ac.jp*

(Received ; accepted )

## Abstract

The edge-on spiral galaxy NGC 4565 was observed for  $\sim 35$  ks with ASCA in the 0.5–10 keV energy band. The X-ray emission was dominated by two bright sources, which can be identified with two point-like X-ray sources seen in the ROSAT HRI image. The observed 0.5–10 keV fluxes of these sources,  $1.7 \times 10^{-12}$  erg s $^{-1}$  cm $^{-2}$  and  $0.7 \times 10^{-12}$  erg s $^{-1}$  cm $^{-2}$ , imply bolometric luminosities of  $1.0 \times 10^{40}$  erg s $^{-1}$  and  $4 \times 10^{39}$  erg s $^{-1}$ , respectively. They exhibit similar spectra, which can be explained by emission from optically thick accretion disks with the inner disk temperature of 1.4–1.6 keV. One of them, coincident in position with the nucleus, shows too low absorption to be the active nucleus seen through the galaxy disk. Their spectra and high luminosities suggest that they are both mass accreting black hole binaries. However the black-hole mass required by the Eddington limit is rather high ( $\geq 50 M_{\odot}$ ), and the observed disk temperature is too high to be compatible with the high black-hole mass. Several attempts are made to solve these problems.

**Key words:** Black hole physics — Galaxies: individual (NGC 4565) — Galaxies: spiral — Galaxies: X-rays

## 1. Introduction

It has long been known (e.g., Fabbiano 1988) that a fair number of nearby spiral galaxies host extremely luminous X-ray sources with apparently point-like appearances, or “ultra-luminous compact X-ray sources” (hereafter ULXs). Their luminosities can reach  $\sim 10^{40}$  erg s $^{-1}$  (e.g., Read et al. 1997), exceeding the Eddington limit for a 1.4  $M_{\odot}$  neutron star almost by two orders of magnitude. A general indication is that they are indeed mass accreting compact objects associated with the host galaxies, rather than background or foreground contaminants (e.g., Fabbiano 1989). The extremely high luminosities of these objects are thought to indicate some extraordinary conditions of them.

Clarifying the nature of ULXs is of great importance, because they strongly influence our understanding of the X-ray emission from normal spiral galaxies. For example, a ULXs located close to the galaxy center would be mistaken for an active galactic nucleus (AGN) of low luminosity. However, the absence of ULXs in the Milky Way and M31 has hampered clear identification of their nature.

Through observations with ASCA (Tanaka et al. 1994), 0.5–10 keV X-ray spectra have been accumulated on a fair number of ULXs (Petre et al. 1994; Takano et al. 1994; Reynolds et al. 1997; Okada et al. 1998; Uno 1997). Although these ASCA spectra exhibit a fair degree of variety, some of them have been fitted successfully with so called multi-color disk blackbody (MCD) model. Such examples include the center source (X-8) of M33 (Takano et al. 1994), the brightest source (source 1) in IC 342 (Okada et al. 1998), and the source X-6 in M81 (Uno 1997). The MCD model describes optically-thick multi-temperature emission from a standard accretion disk (Shakura, Sunyeav 1973) around a black hole. It can be characterized by the highest disk temperature,  $T_{\text{in}}$ , and the size of the accretion disk (Mitsuda et al. 1984; Makishima et al. 1986).

Although these ASCA results provide an important clue to the understanding of ULXs in terms of mass-accreting black holes, in some cases there remains a fundamental problem (Okada et al. 1998) that the measured values of  $T_{\text{in}}$  are uncomfortably high (1.0–1.8 keV). In order to further examine this issue, it is essential to enlarge the sample of such spectral measurements. Accordingly, we here analyze the ASCA data of the nearby edge-on spiral galaxy NGC 4565. We show that it contains two ULXs, one nearly coincident in projection with its nucleus. Furthermore, we confirm that the spectra of these two

sources can be described well by the MCD model with rather high disk temperature.

## 2. Observations and Results

### 2.1. Observation and Data Reduction

NGC 4565 is a spiral galaxy with an almost perfectly edge-on geometry of inclination  $\sim 86^\circ$  (Hummel et al. 1984). It is located at a high galactic latitude ( $b = 86.4^\circ$ ) and an estimated distance of  $\sim 9.7$  Mpc by the Tully-Fisher relation (Tully 1988). Other distance indicators, such as the globular cluster luminosity function, planetary nebula luminosity function, and surface brightness fluctuations, all indicate similar distance of  $\sim 10$  Mpc (Fleming et al. 1995; Simard & Pritchett 1994; Jacoby et al. 1996).

NGC 4565 was observed by ROSAT three times, once with the HRI and twice with the PSPC (Volger et al. 1996). The archival ROSAT HRI image shown in figure 1a is dominated by two point-like X-ray sources, one about  $0/8$  above the galaxy disk while the other coincident in position with the galaxy nucleus within the ROSAT position accuracy of  $\sim 4''$  (Volger et al. 1996; Rupen 1991).

We observed NGC 4565 with ASCA on 1994 May 28. The SIS (Solid State Imaging Spectrometer; Burke et al. 1994; Yamashita et al. 1997) data were acquired in 2CCD/FAINT mode, while the GIS (Gas Imaging Spectrometer; Ohashi et al. 1996; Makishima et al. 1996) data were taken in the standard PH mode.

The SIS data were selected using the following criteria: a) time after passage through the South Atlantic Anomaly (SAA) was greater than 1 minute; b) the object was at least  $10^\circ$  above the night Earth's limb; c) the object was at least  $20^\circ$  above the bright Earth's limb; d) the cutoff rigidity (COR) of cosmic rays was greater than  $6$  GeV/c; and e) time after day night transition was greater than 100 s. We also removed hot and flickering pixels. The GIS data were selected using the following criteria: a) time after SAA was greater than 1 minute; b) the object was at least  $10^\circ$  above the Earth's limb; and c) the cutoff rigidity (COR) was greater than  $6$  GeV/c. We also used the standard rise-time rejection and spread discrimination to remove particle events. After applying these criteria, we obtained  $\sim 31.5$  ks of good SIS data, and  $\sim 35.5$  ks of good GIS data. The galaxy was clearly detected, at counting rates of  $0.08$   $c\ s^{-1}$  (in  $0.5$ – $10$  keV) per SIS detector, and  $0.05$   $c\ s^{-1}$  (in  $0.7$ – $10$  keV) per GIS detector.

## 2.2. X-Ray Images

Figure 1b shows the ASCA SIS (SIS0 plus SIS1) image of NGC 4565 after correcting the attitude data for known temperature effects. The ASCA image comprises two emission peaks with a separation of  $\sim 0.8'$ , presumably corresponding to the two sources visible in the HRI image (figure 1a).

To confirm the presence of the two sources in the ASCA image, we have projected the SIS events inside the rectangle of figure 1b onto its longer side. The derived one-dimensional X-ray profiles are shown in figure 2, in three representative energy bands. Each profile can be fitted well by the projected Point Spread Function (PSF) of the X-ray image convolved with the two point sources, of which the locations are fixed to those determined with the ROSAT HRI. We assumed constant background and determined the intensities of the two sources in the three energy bands, as tabulated in table 1. We can see that intensity ratios of the two sources observed by ASCA are energy independent within the statistical errors. The discrepancy between the ASCA and ROSAT HRI ratios may be due to time variability.

## 2.3. Summed Energy Spectra

Now that the two sources have been confirmed to have similar spectra, we tentatively analyze their spectra together as a first-cut analysis. We hence accumulated the SIS and the GIS events over circular regions of radii  $4'$  and  $6'$  respectively, both centered on the off-center (brighter) source, and obtained the spectra shown in figure 3a. We subtracted background spectra accumulated using a source free region of the same dataset for the SIS, and blank-sky data for the GIS. We fitted these SIS/GIS spectra simultaneously with a common model; either a power-law, a thermal Bremsstrahlung, a plasma emission (Masai 1984), a blackbody, or an MCD model. For the spectral fitting, we used the response function for a point source located at the off-center source.

The fit results are summarized in table 2. Thus, the blackbody model was unsuccessful. The power-law model gives a much better fit with  $\chi^2/\nu = 1.44$ , but the probability of this fit being acceptable is less than 1%. Residuals to the power-law fit indicate that the observed spectra are more convex than a single power-law; even if the two sources have different spectral slopes, their sum would not exhibit such a convex shape. We therefore rule out the power-law fit.

The remaining three models all give acceptable fits to the data. However, the plasma emission fit requires a very low metallicity; therefore it is basically the same as the Bremsstrahlung fit. The Bremsstrahlung model, in turn, requires an intrinsic absorption much exceeding the galactic line-of-sight column density of  $N_{\text{H}} = 1.3 \times 10^{20} \text{ cm}^{-2}$ . Such a moderately absorbed Bremsstrahlung model is known to empirically approximate optically-thick emission arising from accreting non-magnetized compact objects (Makishima et al. 1989), rather than having its own physical meaning. We therefore regard the Bremsstrahlung fit as essentially equivalent to the MCD fit, which is also acceptable. The MCD fit has yielded  $T_{\text{in}} \sim 1.4 \text{ keV}$ , and the 0.5–10 keV flux of the sum of the two sources becomes  $2.3 \times 10^{-12} \text{ erg s}^{-1} \text{ cm}^{-2}$ . The flux is thought to be dominated by the two sources, because the contribution from the underlying ordinary X-ray binaries are estimated to be  $< 10\%$  by assuming that the  $f_{\text{X}}/f_{\text{B}}$  ratio is the same as that of M31 (Makishima et al. 1989), where  $f_{\text{X}}$  represents the X-ray flux and  $f_{\text{B}}$  represents the optical B-band flux.

Although the single MCD fit is acceptable, the observed spectra may contain an additional hard component. For example, if the two sources are low-mass X-ray binaries (LMXBs; close binaries involving non-magnetic neutron stars), we expect to detect a blackbody hard component of temperature  $\sim 2 \text{ keV}$ , arising from the neutron-star surface (Mitsuda et al. 1984). To examine this possibility, we refitted the SIS and GIS spectra with the MCD model plus a blackbody model, with the blackbody temperature fixed at 2.0 keV to ensure a stable fitting. The MCD parameters and the absorption were allowed to float again. However the data did not require the blackbody component, with its 0.5–10 keV flux being  $< 33\%$  (90% confidence) of the total 0.5–10 keV flux. In short, the obtained spectra are considerably softer than those of LMXBs. The result of Bremsstrahlung fit given in table 2 also supports this interpretation, because the Bremsstrahlung approximation to the ASCA spectra of LMXBs usually give a considerably higher temperature of  $8 \sim 13 \text{ keV}$ .

We also repeated the MCD fitting by replacing the blackbody component by a hard power-law with its photon index fixed at 2.2: this simulates the spectra of black-hole binaries in the high (or soft) state (Tanaka, Lewin 1995). The power-law was not required either, with its 0.5–10 keV flux being  $< 35\%$  (90% confidence) of the observed flux in the same range.

#### 2.4. Spectra of Individual Sources

As a further investigation, we attempted to estimate the spectra of the two sources individually. We therefore fitted the same SIS and GIS spectra jointly with a sum of two MCD components having separate temperatures, separate normalizations, and separate column densities, which are all left free to vary. We imposed additional constraints that each MCD component should correctly reproduce the three-band coarse spectrum of the corresponding source, which was produced by converting the count rates in table 1. The response function to represent the three-band spectra was made by scaling and rebinning the response function used in section 2.2. As a result, we fitted four spectra (whole spectrum of SIS, that of GIS, three-band SIS spectrum for the off-center sources, and that for the center source) and determine the model parameter to minimize the total chi-square. In other words, we performed a simultaneous fitting to the spectral and imaging data sets.

This composite model have given an acceptable fit with an overall chi-squared of 147.7 for 124 degree of freedom, and the obtained results are summarized in table 3. Thus, the two sources exhibit the same disk temperature within errors, which in turn agree with that derived in table 2. This justifies our analysis performed in section 2.3. Neither source exhibit detectable absorption, again in agreement with table 2. We repeated the same fitting using different model combinations. When the off-center source spectrum is represented by a power-law, the overall fit becomes unacceptable ( $\chi^2/\nu=159.1/124$ ). In contrast, the center source spectrum was described equally well ( $\chi^2/\nu=143.9/124$ ) when its MCD model is replaced by a power-law model of photon index  $\Gamma = 1.55^{+0.28}_{-0.22}$ . However, the absorption associated with this power-law model for the center source remained rather low ( $\leq 2 \times 10^{21} \text{ cm}^{-2}$ ), with the MCD parameters for the off-center source remained unchanged within the statistical errors.

### 3. Discussion

Using ROSAT and ASCA, we have detected two point-like luminous X-ray sources in the edge-on spiral galaxy NGC 4565. Their spectra have been described successfully by the MCD model with disk temperatures  $T_{\text{in}} = 1.4 - 1.6 \text{ keV}$ , although that of the center source can also be described with a power-law of  $\Gamma = 1.55$ .

### 3.1. The Off-Center Source

The off-center source is the brighter of the two. It locates  $\sim 2$  kpc above the galaxy disk. Since this exceeds the typical scale height ( $\sim 0.2$  kpc) of the X-ray source distribution in Our Galaxy, the source may be suspected to be a background AGN or a foreground object. However, a chance probability to find an X-ray source of 0.5–10 keV flux exceeding  $1 \times 10^{-12}$  erg s $^{-1}$  in a particular sky region encompassing NGC 4565, e.g.,  $2' \times 10'$  in size, is only  $\sim 0.3\%$ , as calculated from the log  $N$ –log  $S$  distribution for extragalactic X-ray sources (e.g., Ueda et al. 1998). Furthermore, none of AGNs are known to exhibit an MCD-type spectrum that has a mildly concave shape in a logarithmic plot. The chance probability of this source being a foreground Galactic object is also quite low, because of its location close to the Galactic north pole. We therefore conclude that this source is associated with NGC 4565.

Applying bolometric correction via the MCD model and employing the 9.7 Mpc distance, the bolometric luminosity of the off-center source becomes  $2.0 \times 10^{40}$  erg s $^{-1}$  if the emission is isotropic, or  $1.0 \times 10^{40} (\cos i_o)^{-1}$  erg s $^{-1}$  if assuming a flat disk geometry with an inclination  $i_o$ . These values much exceed the Eddington limit for a  $1.4 M_\odot$  neutron star.

The high luminosity and a relatively large distance above the galaxy disk suggest that this source belongs to a globular cluster in NGC 4565. However, we would then need some  $\sim 100$  or more LMXBs residing in one or a few globular clusters, with each LMXB radiating at a near-Eddington luminosity. Such a high concentration of luminous LMXBs is never observed in the Milky Way or M31. Furthermore, due to the averaging effect, we would then observe a typical LMXB spectrum, with nearly equal luminosities in the MCD and blackbody components (Mitsuda et al. 1984). This contradicts our results derived in section 2.3, and hence unlikely. We therefore conclude that the off-center source is a ULXs.

### 3.2. The Center Source

At a distance of 9.7 Mpc, the bolometric luminosity of the center source is  $8 \times 10^{39}$  erg s $^{-1}$  for an isotropic emission, or  $4 \times 10^{39} (\cos i_c)^{-1}$  erg s $^{-1}$  for a disk-like emission, where  $i_c$  is the inclination of this object. This also exceeds very much the Eddington limit for a neutron star.

Then, together with its positional coincidence (within  $\sim 0.2$  kpc) with the nucleus of NGC 4565, the

simplest account of the source would be a low-luminosity AGN of NGC 4565. However, the clear detection of this source with the ROSAT HRI (figure 1a) and the ASCA spectral results (table 3) consistently indicate that the absorbing column density to this source is quite low ( $\leq 0.5 \times 10^{21} \text{ cm}^{-2}$  in terms of the MCD model). Even if we assume a power-law model for the center source,  $N_{\text{H}}$  still remains rather low ( $\leq 2.0 \times 10^{21} \text{ cm}^{-2}$ ). On the other hand, judging from the inclination of  $86^\circ$  for NGC 4565 (Hummel et al. 1984), and scaling the absorption column to Our Galaxy center of  $\sim 5 \times 10^{22} \text{ cm}^{-2}$  (Predehl et al. 1994), the column density along the galaxy disk to the nucleus of NGC 4565 would amount at least to  $\sim 1 \times 10^{22} \text{ cm}^{-2}$ . Such a large absorption is ruled out by the data, therefore the center source is not likely to be a low-luminosity AGN. The low absorption also rules out securely this source being a background AGN. Judging from its particular position, this source is not likely to be a foreground object, either. Furthermore, the same argument as conducted in the previous subsection makes this source unlikely to be an assembly of luminous LMXBs. We therefore suggest that the center source is a second ULX in NGC 4565, located at the near-side edge of the disk of the galaxy.

### 3.3. *The Nature of the Two Sources and Associated Problems*

Taking it for granted that the two sources are both ULXs, the clue to their nature may be provided by their spectra. These objects cannot be very luminous Crab-like supernova remnants, since the power-law fit failed to describe the spectrum of the off-center source (§ 2.4), and the photon index of  $\Gamma = 1.55$  for the center source is inconsistent with the typical Crab-type slope of  $\Gamma \sim 2.0$ . As already discussed, the interpretation as an assembly of LMXBs is incompatible with the measured spectra. An X-ray pulsar with a significant radiation beaming is also unlikely, because luminous Galactic and Magellanic X-ray pulsars exhibit significantly flatter continua in the ASCA band, with typical photon indices in the range 0.5–1.2 (Nagase 1989).

In contrast, we have reproduced their 0.5–10 keV spectra successfully by the MCD model (or its empirical approximation by an absorbed thermal Bremsstrahlung model). Furthermore, the MCD model is applicable to the ASCA spectra of three other ULXs as mentioned in section 1. These results indicate that the X-ray emission from these two ULXs, and possibly from some other ULXs too, originate from

optically-thick accretion disks in these objects. These ULXs are therefore inferred to be mass-accreting black holes in the high state, wherein the MCD emission from the accretion disk dominates in the X-ray band. However, as discussed below, this interpretation involves two serious problems.

An immediate problem associated with the black-hole interpretation of ULXs is that the black-hole mass required to satisfy the Eddington limit is quite high. In fact, for the off-center and the center sources to be radiating below the Eddington limit, their black-hole mass has to be

$$M_o^{\text{Ed}} > 73 (\cos i_o)^{-1} M_{\odot}, \quad M_c^{\text{Ed}} > 29 (\cos i_c)^{-1} M_{\odot}, \quad (1)$$

respectively. Black holes as massive as  $M_o^{\text{Ed}}$  have never been observed, and invoking such objects may contradict current understanding of the stellar evolution.

The other, more delicate problem is that the measured values of  $T_{\text{in}}$  of the two ULXs are rather high compared to those of Galactic and Magellanic black-hole binaries (typically 0.5–1.2 keV; Tanaka, Lewin 1995). As first pointed out by Okada et al. (1998) with respect to the ULX in IC 342, this implies a serious self-inconsistency in the black-hole interpretation of ULXs; below, we describe this issue.

The bolometric luminosity of an MCD emission may be described as (Mitsuda et al. 1984; Makishima et al. 1986)

$$L_{\text{bol}} = 4\pi(R_{\text{in}}/\xi)^2\sigma(T_{\text{in}}/\kappa)^4, \quad (2)$$

where  $R_{\text{in}}$  is the innermost radius of the optically-thick accretion disk,  $\sigma$  is the Stefan-Boltzmann constant,  $\kappa \sim 1.7$  (Shimura, Takahara 1995) is ratio of the color temperature to the effective temperature, and  $\xi = (3/7)^{1/2}(6/7)^3 = 0.41$  (Kubota et al. 1998) is a correction factor. By substituting the bolometric luminosities of the two sources, and assuming  $\kappa = 1.7$  and  $\xi = 0.41$ , we may solve equation (2) to obtain  $R_{\text{in}} = 173_{-16}^{+21} (\cos i_o)^{-1/2}$  km and  $R_{\text{in}} = 83_{-22}^{+26} (\cos i_c)^{-1/2}$  km for the off-center and the center sources, respectively.

After previous works (e.g. Dotani et al. 1997), we may identify  $R_{\text{in}}$  with the radius inside which stable Kepler orbits no longer exist. This radius becomes  $3 R_S$  for a non-spinning black hole of mass  $M$ , where  $R_S = 2GM/c^2 = 9.0(M/M_{\odot})$  km is the Schwarzschild radius, with  $G$  the constant of gravity and  $c$  the light speed. We then obtain  $M_o = 19.2_{-1.8}^{+2.4} (\cos i_o)^{-1/2} M_{\odot}$  for the off-center source, and

$M_c = 9.2_{-2.5}^{+2.9} (\cos i_c)^{-1/2} M_\odot$  for the center source. These values considerably fall short of the mass lower limits imposed by equation (1), even if taking the most favourable case of  $i_o = i_c = 0$ . This severe self-inconsistency arises because  $T_{\text{in}}$  is too high, and hence  $R_{\text{in}}$  is too small, for the large black-hole mass required by the high luminosities. Essentially the same problem has been reported by Okada et al. (1998) on the brightest ULX in IC 342.

### 3.4. Possible Solutions to the Problems

We here attempt to solve the two problems raised in § 3.3, that the inferred black-hole mass is too high, and that the disk is too hot. One simple way around these problems is to assume that the black-hole has a reasonable mass, e.g.  $10\text{--}20 M_\odot$ , and the observed high X-ray flux is due to radiation beaming toward us. This hypothesis has often been employed by various authors in a rather ad-hoc way, when discussing the nature of ULXs. However, none of them have successfully presented mechanisms to produce such a radiation beaming. Consequently, we do not appeal to this solution.

Another obvious solution to the issue is to presume that the employed distance to NGC 4565,  $D = 9.7$  Mpc, was significantly over-estimated. However, we do not have a large degree of freedom of changing  $D$ , since various distance estimates consistently yield  $D \sim 10$  Mpc as already mentioned in § 2.1. Here, let us take a rather extreme assumption of  $D = 4.9$  Mpc instead of 9.7 Mpc, and also assume  $i_o = i_c = 0$ . Then, the bolometric luminosities of the two sources become  $2.6 \times 10^{39}$  ergs s $^{-1}$  and  $1.0 \times 10^{39}$  ergs s $^{-1}$ , and hence the mass limits of equation (1) become

$$M_o^{\text{Ed}} > 18 M_\odot, \quad M_c^{\text{Ed}} > 7 M_\odot. \quad (3)$$

These values may be reasonable for stellar-mass black holes. Thus, the issue of too high a black-hole mass might be solved by assuming that the distance to NGC 4565 is over-estimated by a factor of 2, and that the two objects are both face-on systems.

Under these assumptions and from equation (2), we obtain  $R_{\text{in}} = 86.3_{-8.0}^{+10.7}$  km and  $R_{\text{in}} = 41.5_{-11.2}^{+13.1}$  km for the off-center and the center sources, respectively, because  $R_{\text{in}}$  is directly proportional to  $D$ . By identifying these again with  $3 R_S$ , we then obtain  $M_o = 9.6_{-0.9}^{+1.2} M_\odot$  for the off-center source, and  $M_c = 4.6_{-1.2}^{+1.5} M_\odot$  for the center source. These values still remain inconsistent with the mass lower

limits imposed by equation (3).

To solve the remaining inconsistency, we notice that the estimates of  $\kappa$  or  $\xi$  may be modified, because these values must be subject to considerable uncertainties. For this purpose, let us consider Cygnus X-1, the most well studied black-hole binary that is thought to have  $D=2.5$  kpc and  $i \sim 30^\circ$  (Dotani et al. 1997). By employing  $T_{\text{in}} = 0.43$  keV and  $L_{\text{bol}} = 2.4 \times 10^{37}$  ergs s $^{-1}$  measured with ASCA (Dotani et al. 1997), together with  $\kappa = 1.7$  and  $\xi = 0.41$ , and equating again  $R_{\text{in}}$  with  $3 R_S$ , we obtain the black-hole mass of Cygnus X-1 to be  $\sim 10 M_\odot$ . This agrees well with the optically estimated mass,  $10.1_{-5.3}^{+4.6} M_\odot$  (Herereo et al. 1995). From this result, we infer that the combination of  $\xi \times \kappa^2 = 1.18$  which we have been using in equation (2) is reasonable, to within a accuracy of  $\sim \pm 50\%$ .

Given the above argument, let us increase  $\xi \times \kappa^2$  by 50%, from 1.18 to 1.77. (If  $\xi$  is kept constant, this implies  $\kappa = 2.55$ .) Because the mass estimate through equation (2) is directly proportional to  $\xi \times \kappa^2$ , we will then obtain  $M_o = 14.4_{-1.3}^{+1.8} M_\odot$ , and  $M_c = 6.9_{-1.9}^{+2.2} M_\odot$ . Although the mass of the center source becomes consistent with the mass lower limit in equation (3), that of the off-center source still remains inconsistent.

Thus, the second problem pointed out in § 3.3 cannot be solved despite a series of compromising assumptions described above. Of course, the problem would be solved if we appeal to more extreme assumptions, e.g.  $D=3$  Mpc. However, we consider such attempts too artificial. Furthermore, the issue of too high a disk temperature (or too low a black-hole mass derived via  $R_{\text{in}}$ ) is found in other ULXs, including IC 342 source 1 (Okada et al. 1998), and M81 X-6 (Uno 1997) of which the distance is accurately known (Freedman et al. 1994). Essentially the same problem has also been reported from a few Galactic jet sources (Zhang et al. 1997), of which accurate estimates on  $D$ ,  $i$ , and the black-hole mass are available.

These arguments suggest that, in some black holes, the disk temperature can get significantly and systematically higher than is predicted by the standard accretion-disk picture. Zhang et al. (1997) propose that such black holes are spinning rapidly, and the accretion disks are prograde to their rotation; in such a case, the disk can get closer to the black hole, and hence get hotter, just as has been observed. Therefore, the ULXs may be mass-accreting Kerr black holes with several tens solar masses. Further examination of this scenario will be presented elsewhere (Makishima, K., private communication).

Acknowledgement: We thank Dr. T. Hanawa and Dr. K. Nomoto for helpful discussion.

## References

Burke E. B., Mountain R. W., Daniels P. J., Cooper M. J., Dolat V. S. 1994, IEEE Trans. Nucl Sci. 41, 375

Dotani T., Inoue H., Mitsuda K., Nagase F., Negoro H., Ueda Y., Makishima K., Kubota A. et al. 1997, ApJ 485, L87

Fabbiano G. 1988, ApJ 325, 544

Fabbiano G. 1989, ARA&A 27, 87

Fleming D. B., Harris W. E., Pritchett C. J., Hanes D. A. 1995, AJ 109, 1044

Freedman W. L., Hughes S. M., Madore B. F., Mould J. R., Lee M. G., Stetson P., Kennicutt R. C., Turner A. et al. 1994, ApJ 427, 628

Herreiro A., Kudritzki R. P., Gabler R., Vilchez J. M., Gabler A. 1995, A&A 297, 556

Hummel E., Sancisi R., Ekers D. 1984, A&A 133, 1

Jacoby G. H., Ciardullo R., Harris W. E. 1996 ApJ, 462, 1

Kubota A., Tanaka Y., Makishima K., Ueda Y., Dotani T., Inoue H., Yamaoka K. 1998, PASJ 50, 667

Makishima K., Maejima Y., Mitsuda K., Bradt H. V., Remillard R. A., Tuohy I. R., Hoshi R., Nakagawa M. 1986, ApJ 308, 635

Makishima K., Ohashi T., Hayashida K., Inoue H., Koyama K., Takano S., Tanaka Y., Yoshida A. et al. 1989, PASJ 41, 697

Makishima K., Tashiro M., Ebisawa K., Ezawa H., Fukazawa Y., Gunji S., Hirayama M., Idesawa E. et al. 1996, PASJ 48, 171

Masai K. 1984, Ap&SS 98, 367

Mitsuda K., Inoue H., Koyama K., Makishima K., Matsuoka M., Ogawara Y., Shibasaki N., Suzuki K. et al. 1984, PASJ 36, 741

Nagase F. 1989, PASJ 41, 1

Ohashi T., Ebisawa K., Fukazawa Y., Hiyoshi K., Horii M., Ikebe Y., Ikeda H., Inoue H. et al. 1996, PASJ 48, 157

Okada K., Dotani T., Makishima K., Mitsuda K., Mihara T. 1998, PASJ 50, 25

Petre R., Okada K., Mihara T., Makishima K., Colbert E. J. M. 1994, PASJ 46, L115

Predehl P., Trümper J. 1994, A&A 290, L29

Read A. M., Ponman T. J., Strickland D. K. 1997, MNRAS 286, 626

Reynolds C. S., Loan A. J., Fabian A. C., Makishima K., Brandt W. N., Mizuno T. 1997, MNRAS 286, 349

Rupen M. P. 1991, AJ 102, 1

Shakura N. I., Sunyeav R. A. 1973, A&A 24, 337

Shimura T., Takahara F. 1995, ApJ 445, 780

Simard L., Pritchett C. J. 1994, AJ 107, 503

Takano M., Mitsuda K., Fukazawa Y., Nagase F. 1994, ApJ 436, L47

Tanaka Y., Inoue H., Holt S. S. 1994, PASJ 46, L37

Tanaka Y., Lewin W. H. G. 1995, in X-ray Binaries, ed W. H. G. Lewin, J. van Paradijs, W. P. J. van den Heuvel (Cambridge University Press, Cambridge) p126

Tully R. B. 1988, Nearby Galaxies Catalogue. Cambridge University Press, Cambridge

Ueda Y., Takahashi T., Inoue H., Tsuru T., Sakano M., Ishisaki Y., Ogasaka Y., Makishima K. et al. 1998, Nature 391, 866

Uno S. 1997, PhD Thesis, Gakushuin University

Yamashita A., Dotani T., Bautz M., Crew G., Ezuka H., Gendreau K., Kotani T., Mitsuda K. et al. 1997, IEEE Trans. Nucl Sci. 44, 847

Volger A., Pietsch W., Kahabka P. 1996, A&A 305, 74

Zang S. N., Ebisawa K., Sunyaev R., Ueda Y., Harmon B. A., Sazonov S., Fishman G. J., Inoue H. et al. 1997, ApJ 479, 381

Table 1. Observed count rates (in  $10^{-2}$  c s $^{-1}$ ) of the two sources in NGC 4565.\*

Source	ASCA SIS <sup>†</sup>			ROSAT HRI <sup>¶</sup>
	soft <sup>‡</sup>	medium <sup>‡</sup>	hard <sup>‡</sup>	
Off-center .....	1.41 $\pm$ 0.10	1.24 $\pm$ 0.09	0.64 $\pm$ 0.07	0.91 $\pm$ 0.13
Center .....	0.54 $\pm$ 0.09	0.37 $\pm$ 0.07	0.27 $\pm$ 0.06	0.51 $\pm$ 0.09
ratio <sup>§</sup> .....	2.61 $\pm$ 0.47	3.35 $\pm$ 0.68	2.37 $\pm$ 0.59	1.78 $\pm$ 0.40

\* Errors represent one-sigma statistical errors.

† Count rate of the event inside the rectangle, obtained through fitting to the one-dimensional profile of figure 2.

‡ Soft, medium, and hard energy bands correspond to 0.5–1.5, 1.5–3, and 3–10 keV, respectively.

§ Count rate ratio of the off-center source to the center source.

¶ Count rate of the events in circular region of radii 12'', derived from ROSAT HRI archival data.

Table 2. Results of the joint fits to the SIS and GIS spectra of NGC 4565.\* †

Model	absorption ( $10^{21}$ cm $^{-2}$ )	$\Gamma$ or $T$ or $T_{\text{in}}$ (keV)	$\chi^2/\nu$
Power-law .....	2.4 $\pm$ 0.5	1.89 $^{+0.09}_{-0.08}$	174.2/121
Bremsstrahlung .....	1.4 $\pm$ 0.4	5.6 $^{+0.9}_{-0.7}$	152.4/121
Plasma Emission <sup>‡</sup> .....	1.4 $\pm$ 0.4	5.5 $^{+0.9}_{-0.7}$	152.3/120
Blackbody .....	$\leq$ 0.04	0.70 $\pm$ 0.02	335.4/121
MCD .....	$\leq$ 0.2	1.43 $^{+0.07}_{-0.06}$	145.9/121

\* Spectra of the two sources are co-added together.

† Errors represent 90 % confidence limits.

‡ Using the Masai (1984) code. The abundance has been constrained to be  $\leq$  0.1 solar.

Table 3. Estimates of the spectra of individual sources.

Table 1.. Estimates of the spectra of individual sources.

Source	absorption ( $10^{21}$ cm $^{-2}$ )	$T_{\text{in}}$ (keV)	bolometric flux ( $\dagger$ )
Off-center .....	$\leq 0.2$	$1.39 \pm 0.08$	1.82
Center .....	$\leq 0.5$	$1.59_{-0.23}^{+0.32}$	0.72

\* The SIS/GIS spectra of NGC 4565 were fitted jointly with two MCD components, which are constrained to produce the center and off-center source spectrum.

$\dagger$  In unit of  $10^{-12}$  ergs s $^{-1}$  cm $^{-2}$ .

## Figure Captions

Fig. 1. X-ray images of NGC 4565, superposed on the optical (Digital Sky Survey) image (J2000 coordinates). (a) The ROSAT HRI image. (b) The ASCA SIS image in the 0.5–10 keV band. It was smoothed with a Gaussian distribution of  $\sigma = 0'1$ .

Fig. 2. The projected one-dimensional X-ray brightness distribution of NGC 4565, in 0.5–1.5 keV (panel a), 1.5–3 keV (panel b), 3–10 keV (panel c), and 0.5–10 keV (panel d). The SIS events within the rectangle of figure 1b are used. The dotted, dashed, and dot-dashed lines indicate the model for the center-source, that for the off-center source, and a constant background, respectively. The solid histograms show the sum of these three model components, to be compared with the data.

Fig. 3. The SIS and GIS spectra of NGC 4565, dominated by the two sources. The histogram shows the best fit model and the crosses represent the observed spectra. (a) A fit with a single MCD model. (b) A fit with two MCD models, incorporating the constraints that each model can simultaneously reproduce the three-band spectrum (data points with wide bin) of the corresponding source.

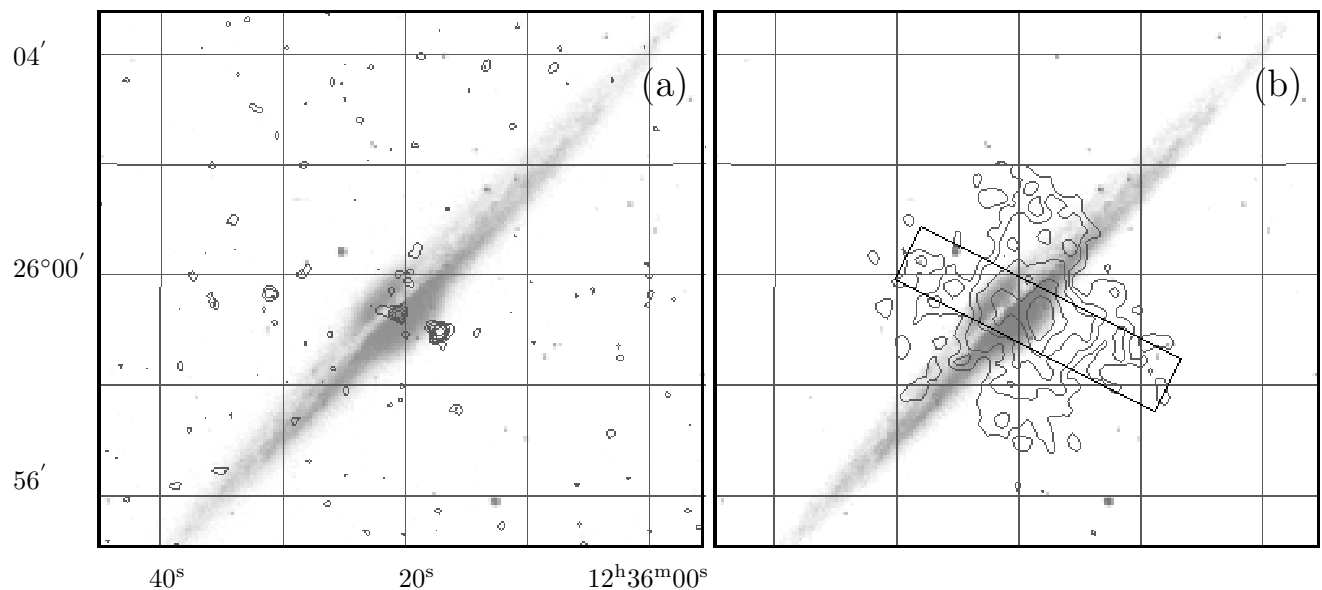


Figure 1

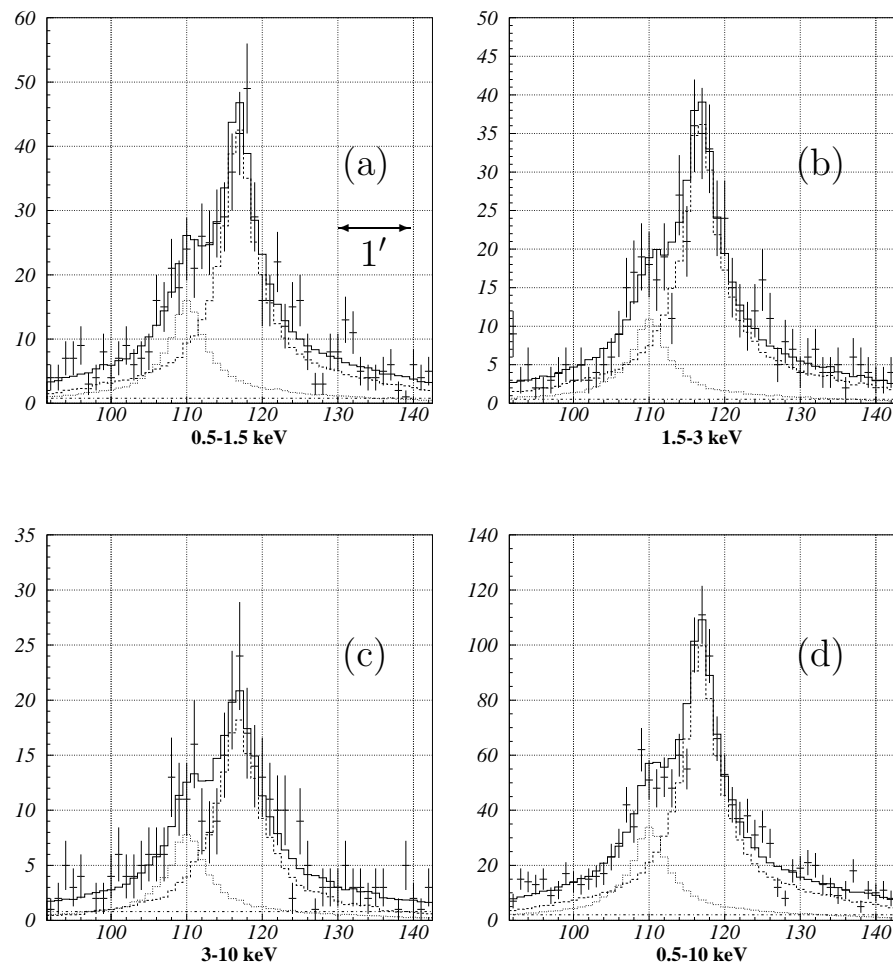


Figure 2

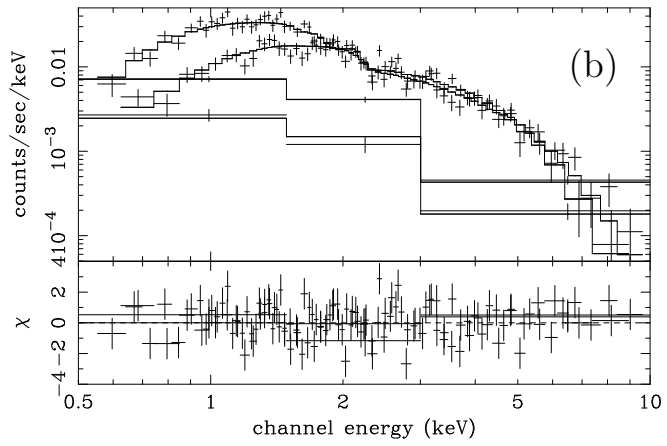
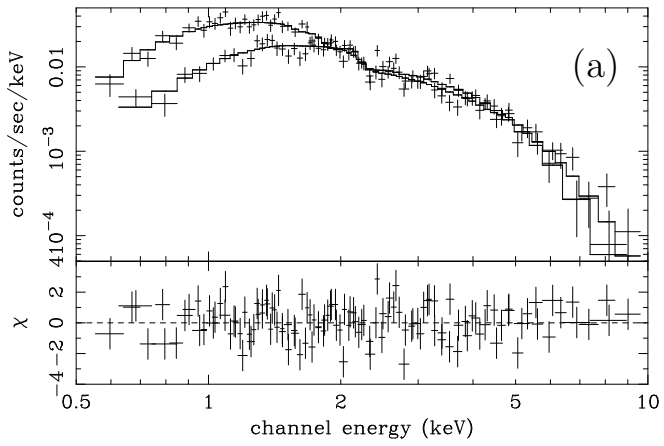


Figure 3